

Fracture Toughness and Fiber Bridging of Carbon Fiber-Reinforced Carbon Matrix Composites

Mototsugu Sakai, Tatsuya Miyajima, and Michio Inagaki
Department of Materials Science, Toyohashi University of Technology,
Tempaku-cho, Toyohashi 440, Japan

ABSTRACT

A fracture mechanics study is reported for two different types of carbon fiber-reinforced carbon matrix composites, a short fiber felt- and a satin woven lamina-composites. It is emphasized prior to discussing their fracture mechanisms that the first matrix cracking is the most substantial fracture process in C/C-composite fracture. Fiber pull-out and bridging processes in the wake region behind the propagating crack tip are discussed using experimental R-curves. The bridging tractions are estimated by the Dugdale model, from which the fiber bridging-enhanced toughening in lamina-composite is demonstrated.

1. INTRODUCTION

Carbon materials have extremely high thermal shock resistance and high chemical stability in non-oxidative environments[1,2]. Furthermore, carbon and graphite materials for high temperature application have the advantage of retained mechanical strength with increasing temperature[2,3], which is contrast to some ceramic and composite materials. Although the fracture toughness of carbon materials (K_{IC}) is less than $1 \text{ MPam}^{1/2}$, being similar to inorganic glasses and glass ceramics, they show appreciable ductility and excellent machinability again in contrast to some of the more brittle ceramic materials. The potential for tailoring mechanical and physical properties over a wide range by changing continuously the crystallographic microstructure[4] from turbostratic (amorphous, glassy) to highly crystalline graphite has been appreciated for applying carbon materials to engineering structures.

The mechanical properties of monolithic carbon and graphite materials can be enhanced through the composite approach[5]. The addition of discrete (chopped) or continuous carbon fibers to carbon matrix effects a synergistic improvement. The matrix combined with fibers produces a material with enhanced performance yielding composites with resistance to failure considerably greater than that of monolithic carbons. "Toughening" is achieved by increasing the fracture energy of carbon composites over what can be attained in the monolithic. In fiber-reinforced composite, crack deflection around the fiber and the increased stress required to break the fiber, i.e., crack impediment in the frontal process zone as well as the fracture

energy consumed by delamination cracking, fiber pull-out, and bridging in the wake region behind the crack tip ensure increased flaw tolerance and pseudo-plasticity (rather than catastrophic failure)[6-11]. Based on these improved mechanical performance in addition to the attractive thermal and high temperature properties, carbon-fiber-reinforced/carbon matrix composites (C/C-composites) have been identified as advanced structural materials for aeropropulsion and space application such as aircraft and missile systems. Driving the state-of-the-art in C/C-composites may be the thermal protection systems for nuclear fusion devices. In particular, C/C-composite tiles have been considered as a viable candidate for the first-wall protection against the thermal shock damage and erosion by nuclear fusion plasma[12].

Depending on the organic precursor and the processing conditions employed, the properties of carbon fibers can be varied over a wide range. Basically, there are three organic precursor materials available as carbon and graphite fibers[5,13]; rayon, polyacrylonitrile (PAN), and pitch (isotropic or mesophase). High elastic modulus (> 300 GPa), high mechanical strength (> 2 GPa) fibers are typically made from PAN or in some cases from mesophase pitch materials, while rayon yields a low elastic modulus (about 25 GPa).

Preform fiber architecture can be classified into four categories, i.e., discrete, continuous (linear, unidirectional), laminated (two-dimensional) and fully integrated (three-dimensional) structures[14]. A discrete fiber system represented

by a short fiber mat or fiber felt, where the fabrics are formed directly from fibers (fiber-to-fabric structures), has no material continuity. Structural integrity is provided mainly by interfiber friction, therefore, the stress transfer between fibers in this fibrous assembly of the reinforcement system is quite low. The reason for using these short fibers is to reduce the anisotropy of integrated architectures. On the other hand, the unidirectional yarns and rovings assemblies (yarn-to-fabric structures) have the highest level of fiber continuity, leading to the highest level of applied load transfer efficiency. However, this fiber architecture is the weakest against intralaminar and interlaminar debonding due to the lack of in-plane and out-of-plane (through thickness) fiber reinforcement. This deficiency is circumvented by planar and/or through-thickness yarn interlacing (weaving), intertwining (braiding), and interlooping (knitting). Thus, because of the wide variety of preform fiber architectures that can be applied to C/C-composites, the mechanical properties can be tailored over a wide range to fit the application.

The carbon matrix placement in these preform fiber architectures is conducted through the carbonization of organic precursors such as phenolic and furfural resins and various types of coal- and petroleum-derived pitch materials, or by the infiltration of pyrolytic carbon using hydrocarbon gas such as natural gas, methane and propane[15,16]. After the initial carbonization, the composite is then subjected to reimpregnation and recarbonization a number of times until the desired density is achieved.

Despite their attractiveness, C/C-composites are not currently being used as much as they could be. Even if they are used, it is in low stress applications, or with such large safety factors as to nullify much of their potential. The reason for this is the difficulty and uncertainty that may exist in defining and determining the materials' strengths, fracture toughness, operating lifetime in service conditions, etc., because of the complicated nature of the deformation and failure behavior. Examples of this behavior include the well-known non-Hookean deformation and hysteresis in the stress-strain relation even below the failure load, prominent mechanical anisotropy, difficulty in determining the onset point of crack initiation, compressive (rather than tensile) fracture in flexural tests, uncertainty in defining fracture toughness and other fracture mechanics parameters, very steep rising R-curve behavior for increasing crack extension, complicated microfracture processes and mechanisms both in the frontal process zone and in the following wake region, etc[6-11]. Hence, despite the fact that the engineering techniques based on linear elastic fracture mechanics (LEFM) have been very successful for assessing and predicting strength, operating lifetime, and reliability of most monolithic materials [17-19], limited success has so far been achieved for composites, in particular, fiber-reinforced composites[20]. There is currently no in-depth understanding of these composites. Because of a serious shortage of reliable data, fracture mechanics models proposed so far are largely based upon conjectures. Attempts to control interface bonding in

fiber-reinforced composites which is essential for tailoring their properties are in their infancy and are largely unguided by present mechanics models.

The key functions of present LEFM are summarized as follows[17-20]; (1) quantitative description of the stress-strain field for a sharp crack or a flaw embedded in an elastic body, and (2) prediction and assessment of strength and lifetime of engineering structures based on a "criterion for fracture". The criterion describing the critical state for a crack to become unstable has its base on an assumption of a "certain" critical value of the stress intensity factor (K) of the crack. It is presumed for the crack to start propagating when the stress intensity equals a "certain" critical value, K_c (fracture toughness). The present LEFM addresses by no means the physical processes and mechanisms of this critical state. None of the atomistic and microstructural discussions on fracture toughness have been conducted in the LEFM regime. It is important to recognize that the fracture criterion of LEFM is merely a hypothesis because of the absence of fracture physics. This LEFM criterion introduces a serious difficulty and confusion to composite fracture although it is successful and plays an important role in predicting fracture behavior of monolithic materials where the fracture toughness in the plane strain condition of these materials is "fortunately" material characteristic. However, the extremely complex fracture of fiber-reinforced composites is outside the LEFM regime. The apparent fracture toughness determined by the LEFM-recipe is strongly dependent on fracture mechanics specimen geometry and

test method, and is never material characteristic. We do not have any rational definition of "toughness" as a material characteristic for these composite materials. Hypnotical application of LEFM to composite fracture with little or no modification never circumvents this serious difficulty. What are needed are more theoretically valid analysis models and quantitative experiments based on a micromechanics viewpoint that recognize the inherent differences in the fracture processes and mechanisms in composite materials.

2. PRELIMINARY CONSIDERATIONS ON THE FRACTURE PROCESSES OF C/C-COMPOSITES

In the absence of a macroscopic notch or crack, it is assumed that failure in a carbon fiber-reinforced carbon matrix composite emanates from small inherent defects or machining-induced surface flaws. These inherent defects may be broken fibers, chopped fibers, flaws and pores in the matrix, and/or debonded fiber/matrix interfaces. Defects in the matrix may lead to matrix cracking between fibers which yield further stress concentrations at the fibers and their interfaces.

Difference in fracture modes of "first fiber cracking" and "first matrix cracking" which occur at the most critical flaw in the fiber or in the matrix under the external applied load is an important consideration for understanding the fracture behavior and strength of composites[10,21,22]. It will be emphasized in what follows, that matrix cracking at the initial stage of the fracture process dominates the failure of C/C-composites, the

same as those of other brittle matrix composites.

Consider, for simplicity, the fracture processes of two different unidirectional carbon fiber reinforced laminae with polypropylene as an extreme of ductile matrix and polycrystalline graphite as representative of a brittle matrix. When a tensile load is applied parallel to the fibers, the strain (ϵ_m) of the matrix will be the same as the strain (ϵ_f) of the fibers if the bond between the fiber and matrix is perfect. The assumption of elastic behavior for both the fiber and the matrix yields a well-known relation referred to as the "rule of mixtures" equation which describes the stress partition between the fibers and the matrix[23];

$$\begin{aligned}\sigma &= \sigma_f v_f + \sigma_m(1 - v_f) \\ &= [E_f v_f + E_m (1 - v_f)] \cdot \epsilon\end{aligned}\quad (1)$$

where σ , ϵ , v , and E stand for stress, strain, volume fraction, and Young's modulus, respectively. The subscripts, f and m , indicate fiber and matrix, respectively. The σ and ϵ in the absence of subscript are of the composite. The stresses distributed in the fibers and the matrix, thus, are given by

$$\sigma_f = E_f \epsilon (= E_f \epsilon_f) = (E_f \sigma) / [E_f v_f + E_m(1 - v_f)] \quad (2a)$$

$$\sigma_m = E_m \epsilon (= E_m \epsilon_m) = (E_m \sigma) / [E_f v_f + E_m(1 - v_f)] \quad (2b)$$

The first cracking stress (the critical stress for the initiation of growth of the most critical flaw (defect) in the fiber or the matrix) is controlled by either the strength of fiber, σ_{fs} (first fiber cracking) or of matrix, σ_{ms} (first matrix cracking), depending on the elastic ratio of matrix to fiber (E_m/E_f). Schematic differences between fiber cracking and matrix cracking are

illustrated in Figs. 1(a) (PAN carbon fiber/polypropylene matrix composite) and Fig. 1(b) (PAN carbon fiber/graphite matrix composite), respectively, where $v_f = 0.5$ is assumed by way of example. The requisite for matrix cracking can be written as

$$\sigma_{ms} < (E_m/E_f) \sigma_{fs} \quad (3)$$

and vice versa for fiber cracking. Using Eq. (3) and mechanical properties for PAN carbon fiber ($E_f = 300$ GPa, $\sigma_{fs} = 3$ GPa), polypropylene ($E_m = 1$ GPa, $\sigma_{ms} = 30$ MPa), and polycrystalline graphite ($E_m = 30$ GPa, $\sigma_{ms} = 30$ MPa) as well as the relations in Figs. 1(a) and 1(b), easily show the first fiber cracking for the C-fiber/polypropylene composite and the first matrix cracking for the C-fiber/graphite composite. Complete bonding at the interface of the fiber/matrix, and no Poisson effects were assumed although these are not strictly true in real composites[23]. More detailed discussions on the matrix cracking in brittle matrix composites have been conducted using failure strains instead of failure stresses[10,21,22].

The preceding application of the rule of mixtures equation to C/C-composite fracture reveals that the first crack appears in, and propagates through, the matrix in the initial stage of the crack growth process. The processes which occur when a sharp matrix crack meets the next fiber are illustrated in Figs. 2(a) and 2(b) for strong and weak interfaces, respectively. It should be noted prior to discussing the matrix crack/fiber interaction that the fracture toughness (K_{IC}) of not only PAN but also mesophase carbon fibers is estimated to be about $1 \text{ MPam}^{1/2}$ from the fracture mechanics studies of various carbon materials;

pyrolytic carbon ($K_{Ic} = 0.93 \text{ MPam}^{1/2}$)[24], glassy carbon ($K_{Ic} = 0.75 \text{ MPam}^{1/2}$)[25,26], and isotropic polycrystalline graphites ($0.75 < K_{Ic} < 1.0 \text{ MPam}^{1/2}$)[27,29]. No appreciable difference in the fracture toughness values between the matrix carbon and the reinforcing fibers and the full maintenance of fiber/matrix continuity as shown in Fig. 2(a) facilitates propagation of the matrix crack into the fiber without the pull-out and bridging of intact fibers along the fracture path. The composite failure is very brittle and catastrophic. The strength of composite in this case is primarily controlled by the first matrix cracking stress.

If the interface region is strong enough for stress transfer, yet weak enough to debond as shown in Fig. 2(b), the matrix crack tip acuity is reduced by the interface debonding. The interfaces blunt the crack tip, significantly alter cracking patterns, and "toughen" the composite. This effect, traditionally recognized among ceramic scientists for centuries, was first formalized by Cook and Gordon[30]. The post-matrix-cracking accompanied by interface debonding leaves extensive fiber pull-out and bridging on the fracture surface behind the propagating crack tip. In other words, C/C-composites with higher "toughnesses" and large strains-to-failure exhibit extensive debonding at the interface. This enhances substantial pull-out of the fiber from the matrix, and yields brushlike fracture surfaces, while C/C-composites with poor "toughness" are fractured by the propagation of a simple crack with smooth surfaces that pass through the matrix and fiber with no evidence of interfacial debonding. These micromechanics results imply that the fiber/matrix interface plays an important role in

determining the "toughness" of unidirectional C/C-composites[31], where the failure is primarily controlled by the first matrix cracking. However, it should be noticed that the associated matrix cracking stress may be substantially greater than the catastrophic fracture stress of the unreinforced matrix carbon[21,22].

A literature survey indicates that only a limited number of systematic and quantitative studies have been reported on fiber-reinforced C/C-composites. Well-established fracture tests, in particular, studies of fracture mechanisms associated with fiber pull-out and bridging in the wake region of the crack are needed to push the usage of fiber-reinforced C/C-composites for structural application.

3. EXPERIMENTAL

Commercial C/C-composites, a CVD-infiltrated carbon fiber felt (CX-2002U, Toyo Tanso Co. Ltd.) and a satin woven lamina composite densified by carbonized phenolic resin (CF222, Schunk Kohlenstofftechnik GMBH) were obtained for this study. In addition, an isotropic fine grain size polycrystalline graphite (IG-11, Toyo Tanso Co. Ltd.) was used as a reference carbon material. Some mechanical and thermal properties are listed in Table 1. Heat-treatment temperature for carbonization and/or graphitization is 3000°C for both the felt-composite and the polycrystalline graphite, and 1700°C for the lamina-composite. The felt-composite was made by first molding the short fiber mat and then infiltrating it using a CVD-process of a hydrocarbon

gas. Mercury porosimetry of the felt composite revealed a rather narrow pore size distribution with the average radius of 8 μm . Thermal conductivity anisotropy ratio is 1.8. On the other hand, the lamina-composite was manufactured to contain 60 vol.% of the woven fabric by first layering, molding and curing the prepregged fabric, and then carbonization and densification. The thickness of each satin woven plane in the composite was about 140 μm .

Fracture testing employed a standard fracture mechanics geometry (Wedge Opening Loaded (WOL) specimen)[32,33] in the opening mode (Mode I) for these composites and fine grain size polycrystalline graphite. The dimensions of WOL-specimen are shown in Fig. 3. The notch-plane of the composites was machined in the edge-wise direction, the nomenclature of which is for the notch plane across the normal planes to either the molding direction or the fabric layers with crack growth direction at a right angle to these planes or layers, approaching the planes (layers) on edge. The notches were diamond sawed in the specimens using a 0.8 mm thickness blade, and then extended about 1 mm with a very thin saw (100 μm) made from a razor blade to finally yield a pseudo sharp crack. The resulting tip radius, \approx 10 μm , was suitable for reliable K_{Ic} measurement. The initial crack depth (a_0) was machined to about 31 mm, i.e., the relative crack length $a_0/W = 0.5$.

Fracture mechanics tests were conducted on an Instron-type testing machine using a cross-head speed of 0.05 mm/min. The load (P) was detected by a load cell. The loadpoint displacement was measured by a clip gage both for the felt-composite and

the polycrystalline graphite. It was estimated from the cross-head displacement for the lamina-composite because of its very large strain-to-failure. The precise measurement of crack length (a) during quasi-static crack extension was required to determine the R-curve in the form of crack growth resistance (K_{R}) versus incremental crack extension (Δa), so that the quantitative observation of the crack tip location during quasi-static crack extension was made on a polished side surface of the test specimen using a traveling microscope (x 50) combined with a video system. The accuracy of crack extension (Δa) measurement was within ± 0.2 mm for the felt-composite and ± 0.05 mm for the polycrystalline graphite. However, because of the complicated fracture processes occurring in the crack tip region of the satin woven lamina-composite, the visual technique was inapplicable not only for identifying the crack tip location but also for determining the precise crack length as well. This difficulty was overcome by introducing a fine drill hole (3 mm in diameter) discrete distances from the initial crack tip along the crack extension path. The load versus displacement relation shows a distinct change when the crack tip meets the hole. It was possible from this change to determine the precise crack length during its extension. The details of the experimental procedure and analysis to determine R-curves, and the correction of the drill hole effect on the crack tip stress field will be reported elsewhere[34].

Saxena and Hudak polynomial formula for the stress intensity factor of WOL-specimen was adopted to calculate K_{R} as a function of crack length[33]:

$$K_I = (P/BW^{1/2})[(2 + a/W)/(1 - a/W)^{3/2}] \\ \times [0.8072 + 8.858(a/W) - 30.23(a/W)^2 \\ + 41.088(a/W)^3 - 24.15(a/W)^4 \\ + 4.951(a/W)^5] \quad (3)$$

The above expression is valid in the range $0.2 < a/W < 1.0$. The accuracy of fit is better than 0.5 percent for linear elastic isotropic materials.

4. RESULTS AND DISCUSSION

4.1 Load versus loadpoint displacement relation

Relations between load (P) and loadpoint displacement (u) of the composites and the fine grain size graphite are shown in Fig. 4 for their quasi-static crack propagation. It is readily seen that the "toughness" which is used here in a very qualitative sense to describe the capacity for withstanding local overstress without catastrophic failure varies in a wide range from the lamina-composite (in the highest) to the fine grain size graphite (in the lowest) and the felt-composite (in between). The arrows in Fig. 4 mark the onset point of the macro-crack extension. The crack initiates at a load far below the peak load in the P-u relation, implying a steep rising R-curve behavior. It is interesting to note that the P-u relations for the carbon materials are appreciably nonlinear at the loads even before the crack initiation, which implies the microscopic failure processes such as microcracking in the matrix carbon, debonding and slip deformation at the fiber/matrix interface, etc. prior to the macro-crack extension. As a matter of fact, a number of acoustic emissions reflecting these micro-failure processes were detected before the macrocrack initiates. The "toughness" can be

evaluated using the work-of-fracture (\mathcal{J}_{wof}) which is calculated from the area under P-u curve[35,36]. The \mathcal{J}_{wof} -values of the lamina-, felt-composites, and the graphite are, respectively, > 6000, 275, and 80 J/m². The value of the lamina-composite is more than 75 times of the isotropic polycrystalline graphite, a superb "toughness" enhancement by woven fabric reinforcement. This "toughening" is mainly caused by the fiber pull-out and bridging processes in the wake region behind the propagating crack tip. A SEM-micrograph demonstrating the fiber pull-out is shown in Fig. 5(a). On the other hand, the "toughness" enhancement in the felt-composite is far less than the lamina-composite. This is illustrated by the rather smooth fracture-surface showing limited fiber pull-out and bridging (Fig. 5(b)). The fiber/matrix interface bonding in the felt-composite appears to be strong enough for the crack to propagate into the fiber. Such a strong bonding at the interface may result from the CVD-infiltration of the matrix carbon.

4.2 Rising R-Curve Behavior

The crack growth resistance curves (R-curve) of the composites and the polycrystalline graphite are shown in Figs. 6(a) and 6(b) expressed as K_R versus Δa . The rising behavior of the fiber composites results certainly from the fiber bridging process. On the other hand, the R-curve of fine grain size polycrystalline graphite is attributed to the crack bridging of the filler grains, the detailed process of which has been discussed by the present authors (MS and MI)[28,37]. In particular, the

rising behavior of the lamina-composite is impressive, with K_R increasing up to $25 \text{ MPam}^{1/2}$ from its initial value (fracture toughness, K_{IC}) of $7 \pm 1 \text{ MPam}^{1/2}$ by the crack extension of 10 mm. In Fig. 6(b), the dotted extrapolation line to $\Delta a = 0$ is drawn by the use of linear extrapolation in Fig. 8(b). The fracture toughnesses (K_{IC}) of the felt-composite and fine grain size graphite are 1.75 and $0.75 \text{ MPam}^{1/2}$, respectively. It should be noticed that the difference in the fracture toughness of our carbon materials is dominated by the micromechanics processes and mechanisms in the process zone ahead of the crack tip (frontal process zone), not by the crack bridging nor contact interactions between fracture surfaces. Of the various toughening processes in frontal process zone, microcracking and crack impediment associated with debonding process at the fiber/matrix interface, and the stress transfer from the matrix to the fiber will be the most significant for carbon composite systems.

The Dugdale model of uniform fiber or grain bridging tractions (σ_b) is adequate for a preliminary consideration of rising R-curve behavior[37-40]. The assumption of uniform bridging tractions has been advanced for some ceramic materials and composites[28,37]. A schematic of crack bridging is depicted in Fig. 7. A fracture mechanics result for the change in observed crack growth resistance, $\Delta K(a)$ ($= K_R(a) - K_{IC}$), is expressed by[38]

$$\Delta K = \sigma_b (\pi a_0)^{1/2} (2/\pi) \arccos [1 - (\Delta a/a_0)] \quad (4)$$

where a_0 is the initial crack length, and Δa is the crack extension ($= a - a_0$). When the bridging zone length, i.e., the crack extension, Δa , is enough smaller than the total crack length, a , Eq. (4) is approximated by[28,37,40]

$$\Delta K = [4 \sigma_b / (2\pi)]^{1/2} (\Delta a)^{1/2} \quad (5)$$

The accuracy of Eq. (5) is within 10 % of the true value yielded by Eq. (4) unless $\Delta a/a$ becomes larger than 0.5. Noting the linear relation of ΔK with $(\Delta a)^{1/2}$ in Eq. (5), the bridging traction, σ_b , can be estimated by the use of the experimental R-curves in Figs. 6(a) and 6(b) as the plots of K_R versus $(\Delta a)^{1/2}$, if the assumption of uniform bridging tractions holds for these carbon materials. The plots are demonstrated in Figs. 8(a) and 8(b), showing excellent linear relations between K_R and $(\Delta a)^{1/2}$ in the initial stage of crack extension. The slope of the rising linear portion gives the bridging tractions, $\sigma_b = 8, 7, \text{ and } 130$ MPa for the fine grain size graphite, short fiber felt-, and the lamina-composites, respectively.

The stress shielding effect of crack bridging reduces the stress concentration at the crack tip and makes the material notch- or flaw-insensitive and damage tolerant. One of the possible expressions for describing notch-sensitivity may be given by the ratio (r) of the tensile strength (σ_t) of the material and its bridging traction (σ_b), i.e., σ_t / σ_b , because the tensile strength is the critical stress of the material in the absence of macro-notch or macro-crack. In an extreme of notch sensitivity, that is, in a case of no bridging, the ratio, r , becomes infinitely large. This is the case of a sharp notch without any stress shieldings. The other extreme is of $\sigma_t \approx \sigma_b$, i.e., $r \approx 1$, in which the stress concentration at notch tip is extinguished through a complete stress shielding by crack bridging. The r -ratios of the carbon materials studied in the

present work are **3.0**, **7.9**, and about 1.0 for the fine grain size graphite, felt- and the lamina-composites, respectively, recognizing the excellent stress shielding and notch tolerance in the lamina-composite.

4.3 Essential Work-of-Fracture

The work-of-fracture (\mathcal{J}_{wof}), which is defined as the total energy consumed to produce a unit area of fracture surface during stable fracture, is one of the most useful nonlinear fracture parameters in the field of nonlinear fracture where LEFM loses its potential. The work-of-fracture has been widely applied to characterize the crack growth resistance for complicated fracture processes such as those of refractory composites[41]. Because of the ambiguous physical meaning, however, the importance of the work-of-fracture parameter has not been appreciated by the fracture mechanics community per se. The fracture mechanics consideration on the work-of-fracture as linked to the J-integral of the materials showing R-curve behavior was first conducted by the present author (MS) [28,29,37]. In general, the work-of-fracture is not a material characteristic, but depends on the specimen geometry unless the dimensions of test specimen is much larger than the process zone size.

Mai and his co-workers demonstrated the importance of the essential work-of-fracture (\mathcal{J}_e) through the extensive studies of the dependence of \mathcal{J}_{wof} for various engineering materials on the remaining ligament length (b) of fracture mechanics specimens[42-47]. They related the \mathcal{J}_{wof} dependence to the nonlinear contribution of large scale frontal process zone. They proposed

an important linear relation between \mathcal{K}_{wof} and the ligament length, b [42-47];

$$\mathcal{K}_{wof} = \mathcal{K}_e + Ab \quad (6)$$

where A is a numerical constant describing the dimension of the frontal process zone.

The dependence of \mathcal{K}_{wof} on b is shown in Figs. 9(a) and 9(b) for these carbon materials. In order to obtain the relations shown in Fig. 9, a number of WOL-specimens with different initial crack lengths (a_0), i.e., with different ligament lengths (b), were prepared for fracture tests. It is readily seen that the linear relation between \mathcal{K}_{wof} and b exists as well in our crack bridging systems. Combining the essential work-of-fracture, \mathcal{K}_e , which is determined by the linear extrapolation to $b = 0$ in Fig. 9, and the well-known Irwin's relation[17-20], $K_{IC} = (2 \mathcal{K}_e E)^{1/2}$, the fracture toughnesses estimated are 0.9, 2.3, and 13 MPam^{1/2} for the polycrystalline graphite, felt- and the lamina-composites, respectively, having close values to those determined from the critical stress intensity factor. The fracture mechanics consideration on the linear relation between \mathcal{K}_{wof} and b in crack bridging and microcracking systems, the fracture physics of \mathcal{K}_e , and the related fracture mechanisms will be reported elsewhere in detail[34].

5 CONCLUDING REMARKS

Mechanical properties of carbon fiber-reinforced carbon matrix composites can be tailored over a wide range to fit their application to various engineering structures because of the wide variety of preform fiber architectures for reinforcement and of various crystallographic carbon microstructures available. The major advantage of carbon and carbon composites is the full maintenance of mechanical strength over 1500°C in non-oxidative environments.

Because of the brittle nature of the matrix carbon, the first cracking which occurs at the most critical flaw in the matrix determines the strength of C/C-composites. If the matrix/fiber interface bonding is perfect, the matrix crack propagates into fibers without leaving intact fibers to produce pull-out and crack bridging along the fracture path, resulting in no-toughening in the wake region. However, provided that the interface region is strong enough for stress transfer, yet weak enough to debond, the interfaces blunt the crack tip, significantly alter cracking patterns, yield extensive fiber pull-out and bridging, and toughen the composite.

Two different types of C/C-composites, a short fiber felt- and satin woven lamina-composites, and a fine grain size isotropic polycrystalline graphite were obtained for fracture mechanics study. Precise measurements of rising R-curves for these carbon materials were conducted using wedge opening loaded (WOL) specimens. The rising R-curve behavior of felt- and lamina-composites was primarily caused by the fiber bridging on the

fracture surfaces, while the crack bridging by filler grains in the wake region was dominant for the fine grain size polycrystalline graphite. Because of a very strong bonding between the fiber and CVD-infiltrated matrix in the felt-composite, it yielded rather smooth fracture surfaces with very limited fiber bridging, the bridging traction of which is as small as that of the polycrystalline graphite. On the other hand, the fiber pull-out and bridging in the lamina-composite was very extensive, resulting in brushlike fracture surfaces. The crack growth resistance (K_R) increased from its initial value (K_{Ic}) of about $7 \text{ MPam}^{1/2}$ to $25 \text{ MPam}^{1/2}$ by 10 mm crack extension. The fiber bridging traction (= 130 MPa) of the lamina-composite is about the same as its tensile strength, implying a superb stress shielding at the crack tip and excellent notch tolerance. The important role of matrix/fiber interface bonding was emphasized through the present work.

Acknowledgments: A part of the present work was supported by a Grant-in-Aid for Nuclear Fusion Research (# 62050002) from the Japanese Ministry of Education. The authors are grateful to Toyo Tanso Co. Ltd. and Schunk Kohlenstofftechnik GMBH for the preparation of C/C-composites. Helpful comments of M.G. Jenkins with Oak Ridge National Laboratory are greatly acknowledged.

REFERENCES

- 1) Z. Zudans, T.C. Yen, and W.H. Steingelman, Thermal Stress Techniques in the Nuclear Industry, Elsevier, New York, 1965.
- 2) W.R. Reynolds, Physical Properties of Graphite, Elsevier, London, 1968.
- 3) B.T. Kelly, Physics of Graphite, Applied Science Publishers, London, 1981.
- 4) E.I. Shobert II, "Carbon and Graphite", pp. 1-99 in Modern Materials, Vol. 4, Academic Press, New York, 1964.
- 5) J.D. Buckley, "Carbon-Carbon, An Overview", Ceram. Bull., 67[2]364-68(1988).
- 6) J. Guo, Z. Mao, C. Bao, R. Wang, and D. Yau, "Carbon Fiber-Reinforced Silicon Nitride Composites", J. Mater. Sci., 17, 3611-15(1982).
- 7) K.M. Prewo, "Fiber-Reinforced Ceramics: New Opportunities for Composite Materials", Ceram. Bull., 68[2]395-400(1989).
- 8) D.B. Marshall and A.G. Evans, "Failure Mechanisms in Ceramic-Fiber/Ceramic-Matrix Composites", J. Am. Ceram. Soc. 68[5]225-32(1985).
- 9) D.B. Marshall, B.N. Cox, and A.G. Evans, "The Mechanics of Matrix Cracking in Brittle-Matrix Fiber Composites", Acta metall., 23[11]2013-21(1985).
- 10) M.D. Thouless and A.G. Evans, "Effects of Pull-Out on The Mechanical Properties of Ceramic-Matrix Composites", Acta metall., 36[3]517-22(1988).
- 11) A.G. Evans, "The New Generation of High Toughness Ceramics", pp. 775-794 in Ceramic Microstructures '86; Role of Interface, Edited by J.A. Pask and A.G. Evans, Plenum, New York, 1987.
- 12) M.J. Davis, "Design with Brittle Materials", pp. 214-232 in Proceedings of P115, The First Japan-US Workshop on Advanced Ceramics for Fusion Application, Edited by K. Kawamura, et al, Tokyo, 1988.
- 13) D.J. Johnson, "Recent Advances in Studies of Carbon Fiber Structure", Phil. Trans. R. Soc. London, A294, 443-49(1980).
- 14) F.K. Ko, "Preform Fiber Architecture for Ceramic Matrix Composites", Ceram. Bull., 68[2]1401-14(1989).
- 15) J.C. Bokros, "Deposition Structure and Properties of Pyrolytic Carbon", pp. 1-118 in Chemistry and Physics of Carbon, Vol. 5, Edited by P.L. Walker, Marcel Dekker, New York, 1969.
- 16) W.H. Smith and D.H. Leeds, "Pyrolytic Graphite", pp. 139-221 in Modern Materials, Vol. 7, Academic Press, New York, 1970.
- 17) D. Broek, Elementary Engineering Fracture Mechanics, Nijhoff, The Hague, 1982.
- 18) R.W. Hertzberg, Deformation and Fracture Mechanics of Engineering Materials, Wiley, New York, 1983.
- 19) S.T. Rolfe and J.M. Barson, Fracture and Fatigue Control in Structures-Application of Fracture Mechanics, Prentice-Hall, New Jersey, 1977.
- 20) M.F. Kanninen and C.H. Popelar, Advanced Fracture Mechanics, Oxford Engineering Science Series 15, Oxford University Press, New York, 1985.

- 21) J. Aveston, G. Cooper, and A. Kelly, "Single and Multiple Fracture", pp. 15-26 in *The Properties of Fiber Composites*, NPL-Conference Proceedings, IPC Science and Technology Press, Guildford, England, 1971.
- 22) B. Budiansky, J.W. Hutchinson, and A.G. Evans, "Matrix Fracture in Fiber-Reinforced Ceramics", *J. Mech. Phys. Solids*, 34[2]167-89(1986).
- 23) D. Hull, *An Introduction to Composite Materials*, Cambridge University Press, Cambridge, 1981.
- 24) M. Sakai, R.C. Bradt, and D.B. Fischbach, "Fracture Toughness Anisotropy of a Pyrolytic Carbon", *J. Mater. Sci.*, 21, 1491-1501(1986).
- 25) J.J. Mecholsky, S.W. Freiman, and R.W. Rice, "Fracture Surface Analysis of Ceramics", *J. Mater. Sci.*, 11, 1310-19(1976).
- 26) T. Miyajima, M. Inagaki, and M. Sakai, unpublished data.
- 27) M. Sakai, K. Urashima, and M. Inagaki, "Energy Principle of Elastic-Plastic Fracture and Its Application to the Fracture Mechanics of a Polycrystalline Graphite", *J. Am. Ceram. Soc.*, 66[12]868-74(1983).
- 28) M. Sakai, J. Yoshimura, Y. Goto, and M. Inagaki, "R-Curve Behavior of a Polycrystalline Graphite: Microcracking and Grainbridging in the Wake Region", *J. Am. Ceram. Soc.*, 71[8]609-16(1988).
- 29) M. Sakai, "Fracture Mechanics and R-Curve Behavior of Graphite Materials", *Tanso*, 1988(No. 134)211-223.
- 30) J. Cook and J.E. Gordon, "A Mechanism for the Control of Crack Propagation in All Brittle Systems", *Proc. R. Soc. London*, A-282, 508-20(1964).
- 31) R.J. Kerans, R.S. Hay, N.J. Pagano, and T.A. Parthasarathy, "The Role of the Fiber-Matrix Interface in Ceramic Composites", *Ceram. Bull.*, 68[2]429-42(1989).
- 32) *Stress Intensity Factors Handbook*, Vol.1, Edited by Y. Murakami, et al., Pergamon, Oxford, 1987.
- 33) A. Saxena and S.J. Hudak, Jr., "Review and Extension of Compliance Information for Common Crack Growth Specimens", *Int. J. Fract.*, 14[5]453-68(1978).
- 34) T. Miyajima, M. Inagaki, and M. Sakai, to be submitted to *J. Am. Ceram. Soc.*
- 35) J. Nakayama, "Direct Measurement of Fracture Energies of Brittle Heterogeneous Materials", *J. Am. Ceram. Soc.*, 48[11]583-87(1965).
- 36) H.G. Tattersal and G. Tappin, "Work of Fracture and Its Measurement in Metals, Ceramics, and Other Materials", *J. Mater. Sci.*, 1[3]296-301(1966).
- 37) M. Sakai and R.C. Bradt, "The Crack Growth Resistance Curve of Non-Phase-Transforming Ceramics", *J. Ceram. Soc. Japan*, 96[8]801-09(1988).
- 38) G.C. Sih, *Handbook of Stress Intensity Factors*, Lehigh University Press, Bethlehem, PA, 1973.
- 39) A.G. Evans and R.M. McMeeking, "On the Toughening of Ceramics by Strong Reinforcements", *Acta metall.*, 34[12]2435-41(1986).
- 40) P.F. Becher, C-H. Hsueh, P. Angelini, and T.N. Tiegs, "Toughening Behavior in Whisker-Reinforced Ceramic Matrix Composites", *J. Am. Ceram. Soc.*, 71[12]1050-61(1988).

- 41) J. Homeny, T. Darroudi, and R.C. Bradt, "J-Integral Measurements of the Fracture of 50% Alumina Refractories", *J. Am. Ceram. Soc.*, 63[5-6]326-31(1980).
- 42) Y-W. Mai and K.M. Pilko, "The Essential Work of Plane Stress Ductile Fracture of a Strain-Aged Steel", *J. Mater. Sci.*, 14, 386-94(1979).
- 43) Y-W. Mai and B. Cotterell, "Effects of Pre-Strain on Plane Stress Ductile Fracture in α -Brass", *J. Mater. Sci.*, 15, 2296-2306(1980).
- 44) B. Cotterell, E. Lee, and Y-W. Mai, "Mixed Mode Plane Stress Ductile Fracture", *Int. J. Fract.*, 20, 243-50(1982).
- 45) Y-W. Mai and B. Cotterell, "The Essential Work of Fracture for Tearing of Ductile Metals", *Int. J. Fract.* 24, 229-36(1984).
- 46) Y-W. Mai and B. Cotterell, "Effect of Specimen Geometry on the Essential Work of Plane Stress Ductile Fracture", *Eng. Fract. Mech.* 21[1]123-28(1985).
- 47) Y-W. Mai and B. Cotterell, "On the Essential Work of Ductile Fracture in Polymers", *Int. J. Fract.* 32, 105-25(1986).

Table 1 Some properties of carbon materials.

	density (g/cm^3)	fiber volume fraction (%)	Young's modulus (GPa)	flexural strength (MPa)	porosity (%)	thermal conductivity (W/m deg)
Fine Grain Size Isotropic polycrystalline Graphite (IG-11)	1.76	0.0	9.0	35	15	120
Felt-Composite (CX-2002U)	1.70	10	12 (//)	55 (flat-wise)	20	325 (//)
Lamina-Composite (CF 222)	1.63	60	45 (//)	200 (flat-wise)	10	-

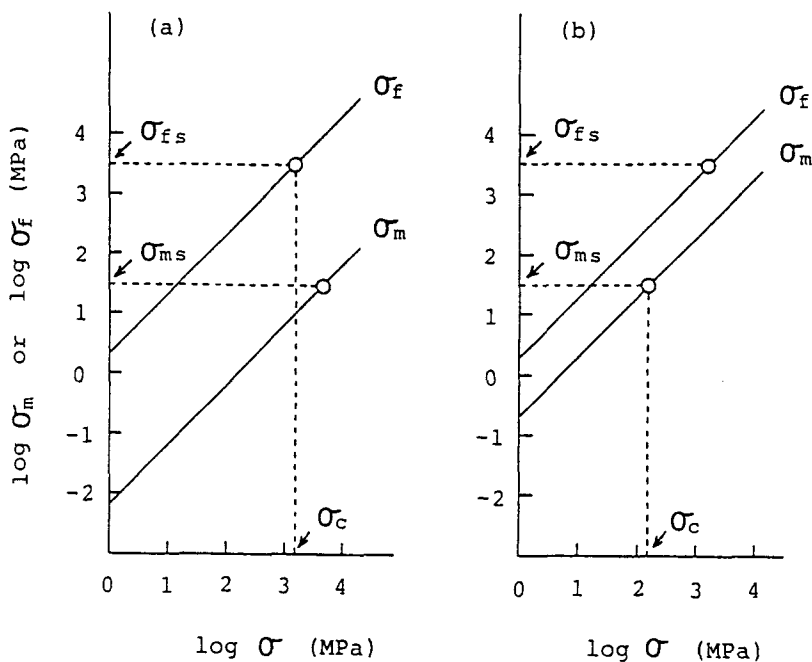


Figure 1 Schematic difference between (a) first fiber cracking (PAN-carbob fiber/polypropylen-matrix) and (b) first matrix cracking (PAN-carbon fiber/graphite-matrix). The stresses distributed in the fibers (σ_f) and in the matrix (σ_m) are logarithmically plotted against the composite stress (σ) with the fiber volume fraction of 0.5. σ_c stands for the first cracking stress of the composite.

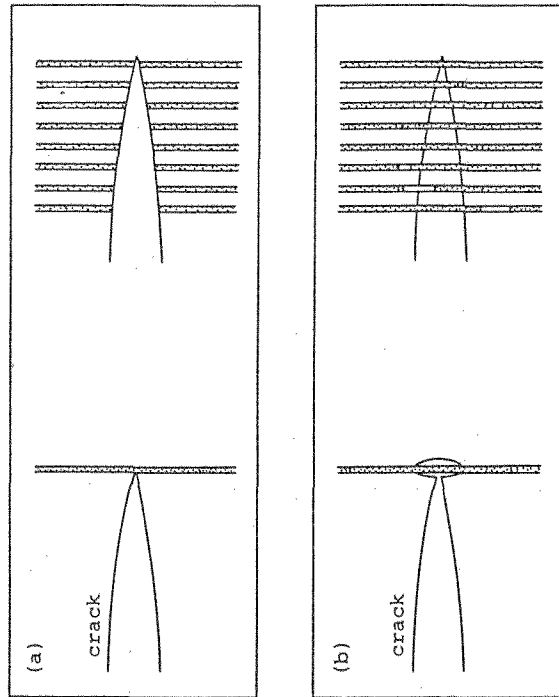


Figure 2 Interaction of a crack with fibers for (a) strong and for (b) weak interfaces.

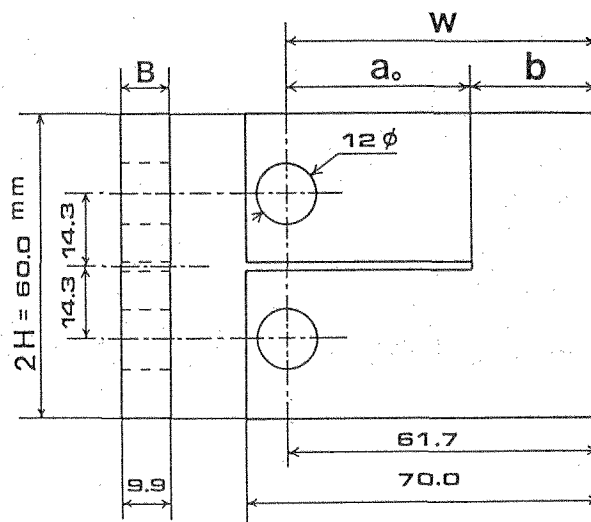


Figure 3 The dimensions of Wedge Opening Loaded specimen.

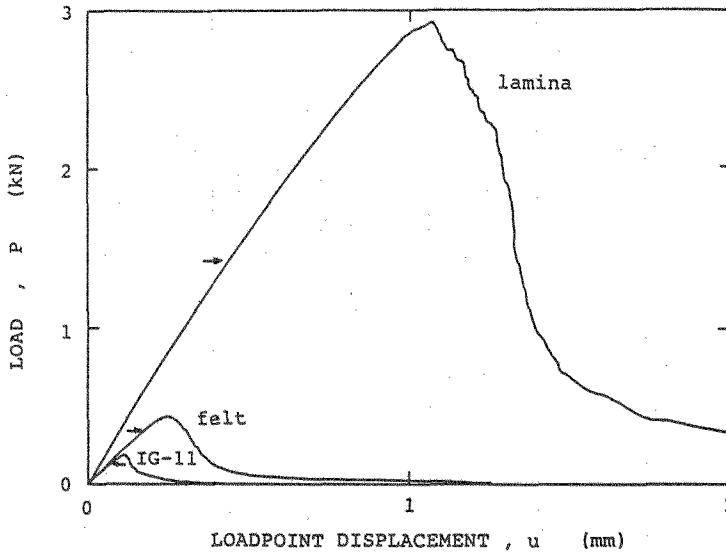


Figure 4 Load (P) versus loadpoint displacement (u) relations for a lamina- and felt-composites, and a fine grain size isotropic polycrystalline graphite during quasi-static crack extension. Arrows mark the onset load of macrocrack extension.

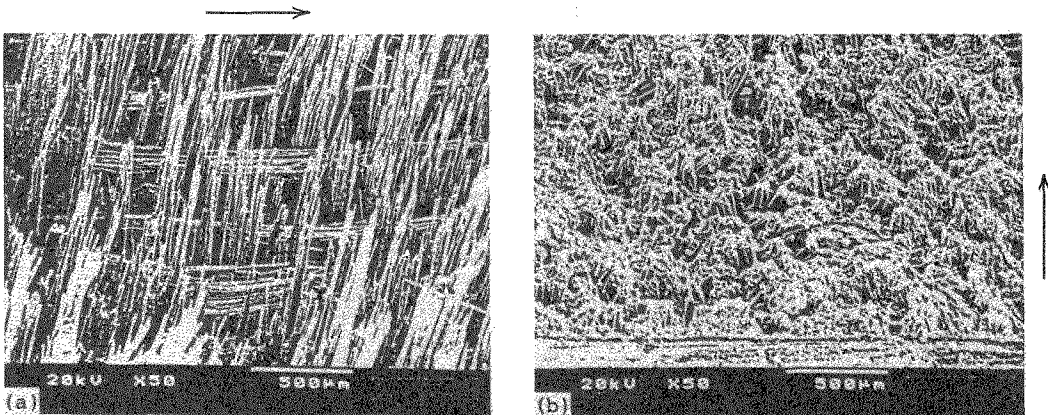


Figure 5 SEM micrographs of the fracture surfaces of (a) lamina- and (b) felt-composites. Arrows show the direction of crack extension.

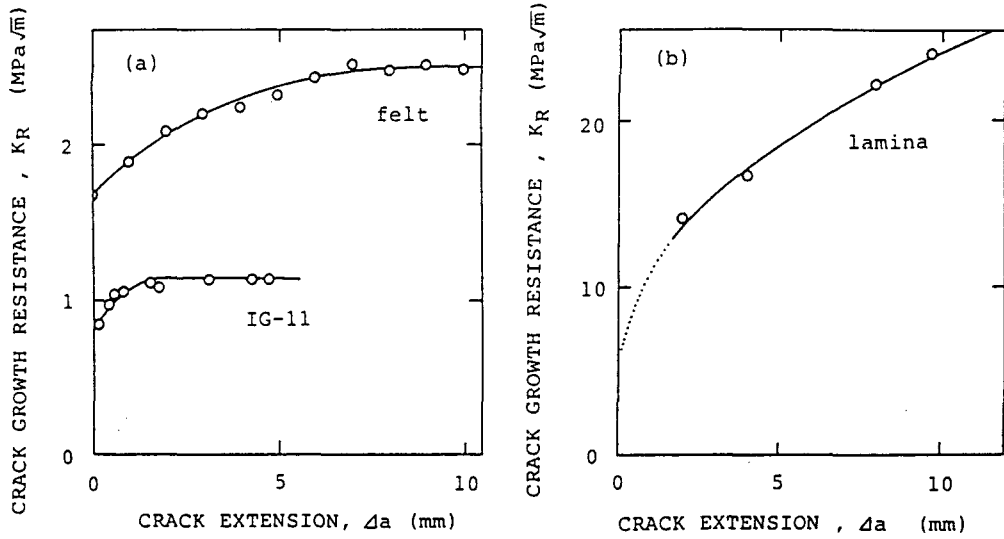


Figure 6 Crack growth resistance curves (R-curves) of carbon and C/C-composites. The dotted extrapolation line in (b) is drawn using the linear extrapolation in Fig. 8(b).

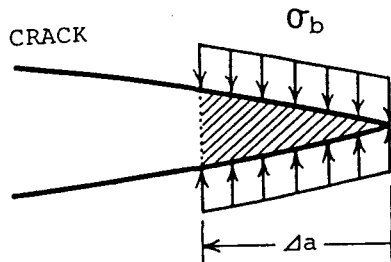


Figure 7 Schematic of uniform crack-bridging tractions (σ_b).

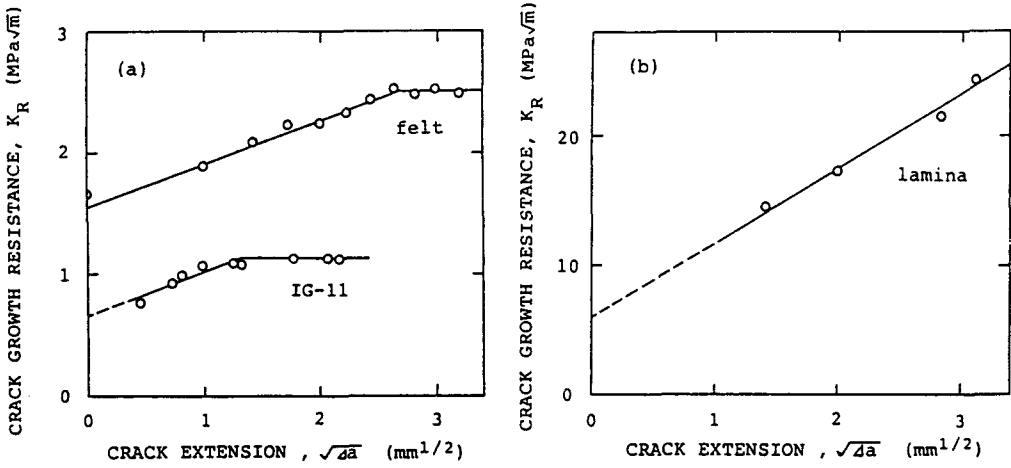


Figure 8 R-curves plotted as K_R versus Δa . The slope of rising linear portion yields the crack-bridging traction (σ_b).

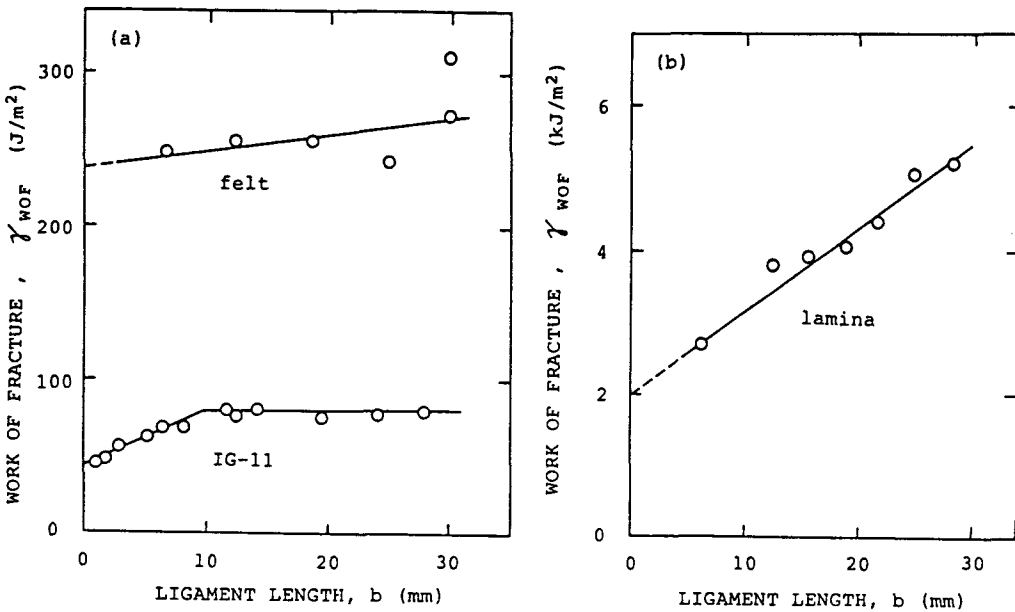


Figure 9 The relations between work-of-fracture (γ_{wof}) and the remaining ligament length (b) of WOL-specimens. A linear extrapolation to $b = 0$ gives the essential work-of-fracture.